US006662033B2

(12) **United States Patent**
Casciani et al.

(10) **Patent No.: US 6,662,033 B2**
(45) **Date of Patent: *Dec. 9, 2003**

(54) **PULSE OXIMETER AND SENSOR OPTIMIZED FOR LOW SATURATION**

(75) Inventors: **James R. Casciani**, Cupertino, CA (US); **Paul D. Mannheimer**, Belmont, CA (US); **Steve L. Nierlich**, San Leandro, CA (US); **Stephen J. Ruskewicz**, Kensington, CA (US)

(73) Assignee: **Nellcor Incorporated**, Pleasanton, CA (US)

(*) Notice: Subject to any disclaimer, the term of this patent is extended or adjusted under 35 U.S.C. 154(b) by 10 days.

This patent is subject to a terminal disclaimer.

(21) Appl. No.: **09/882,371**

(22) Filed: **Jun. 14, 2001**

(65) **Prior Publication Data**

US 2002/0082489 A1 Jun. 27, 2002

Related U.S. Application Data

(63) Continuation of application No. 09/003,413, filed on Jan. 6, 1998, now Pat. No. 6,272,363, which is a continuation of application No. 08/413,578, filed on Mar. 30, 1995, now Pat. No. 5,782,237, which is a continuation-in-part of application No. 08/221,911, filed on Apr. 1, 1994, now Pat. No. 5,421,329.

(51) **Int. Cl.**[7] **A61B 5/00**
(52) **U.S. Cl.** **600/338**; 600/323
(58) **Field of Search** 600/322–323, 600/338, 309–310, 313

(56) **References Cited**

U.S. PATENT DOCUMENTS

3,638,640	A	2/1972	Shaw
3,847,483	A	11/1974	Shaw et al.
4,114,604	A	9/1978	Shaw et al.
4,223,680	A	9/1980	Jobsis
4,623,248	A	11/1986	Sperinde
4,700,708	A	10/1987	New, Jr. et al.
4,714,341	A	12/1987	Hamaguri et al.
4,859,057	A	8/1989	Taylor et al.

(List continued on next page.)

FOREIGN PATENT DOCUMENTS

EP	0 522 674 A2	1/1993
GB	1 595 206	8/1981
GB	1 595 207	8/1981
WO	WO 92/21283 A	10/1992

OTHER PUBLICATIONS

"*Physio–optical considerations in the design of fetal pulse oximetry sensors*", P.D. Mannheimer et al., European Journal of Obstetrics & Gynecology and Reproductive Biology 72 Suppl. 1 (1997) S9–S19.

(List continued on next page.)

Primary Examiner—Eric F. Winakur
Assistant Examiner—Matthew J Kremer
(74) *Attorney, Agent, or Firm*—Townsend and Townsend and Crew, LLP

(57) **ABSTRACT**

A pulse oximeter sensor with a light source optimized for low oxygen saturation ranges and for maximizing the immunity to perturbation induced artifact. Preferably, a red and an infrared light source are used, with the red light source having a mean wavelength between 700–790 nm. The infrared light source can have a mean wavelength as in prior art devices used on patients with high saturation. The sensor of the present invention is further optimized by arranging the spacing between the light emitter and light detectors to minimize the sensitivity to perturbation induced artifact. The present invention optimizes the chosen wavelengths to achieve a closer matching of the absorption and scattering coefficient products for the red and IR light sources. This optimization gives robust readings in the presence of perturbation artifacts including force variations, tissue variations and variations in the oxygen saturation itself.

21 Claims, 14 Drawing Sheets

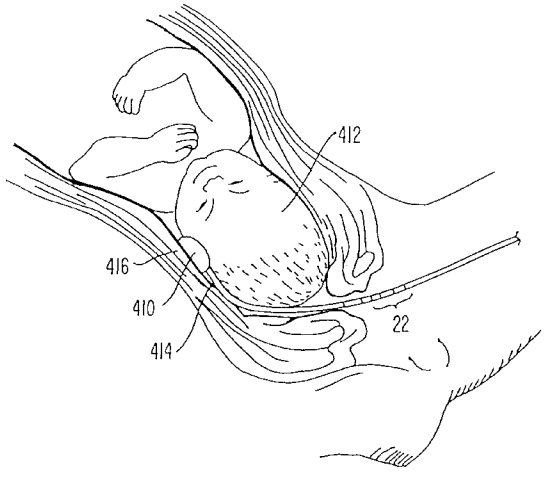

U.S. PATENT DOCUMENTS

4,908,762	A	*	3/1990	Suzuki et al.	364/413.09
4,938,218	A		7/1990	Goodman et al.	
4,975,581	A		12/1990	Robinson et al.	
5,109,849	A		5/1992	Goodman et al.	
5,188,108	A		2/1993	Secker	
5,247,932	A		9/1993	Chung et al.	
5,299,570	A		4/1994	Hatschek	
5,355,880	A		10/1994	Thomas et al.	
5,385,143	A		1/1995	Aoyagi	
5,413,100	A		5/1995	Barthelemy et al.	
5,419,321	A		5/1995	Evans	
5,421,329	A		6/1995	Casciani et al.	
5,424,545	A	*	6/1995	Block et al.	250/343
5,482,036	A		1/1996	Diab et al.	
5,494,032	A	*	2/1996	Robinson et al.	600/323
5,497,769	A		3/1996	Gratton et al.	
5,772,589	A		6/1998	Bernreuter	
5,782,237	A	*	7/1998	Casciani et al.	600/476
5,782,756	A		7/1998	Mannheimer	
6,272,363	B1	*	8/2001	Casciani et al.	600/322
6,298,253	B1	*	10/2001	Buschmann	600/338

OTHER PUBLICATIONS

"*Wavelength Selection for Low–Saturation Pulse Oximetry*", Paul D. Mannheimer et al., IEEE Transaction on Biomedical Engineering, vol. 44, No. 3, Mar. 1997.

"*Noninvasive Optical Monitoring*", Ross Flewelling, The Biomedical Engineering Handbook, CRC Press 1995.

"*Continuous, Non–Invasive Measurements of Arterial Blood Oxygen Levels*", Edwin B. Merrick et al., Hewlett–Packard Journal, Oct. 1976.

"*Noninvasive, Infrared Monitoring of Cerebral and Myocardial Oxygen Sufficiency and Circulatory Parameters*", Frank F. Jobsis, Science—Dec. 23, 1977.

"*Spectral transmittance and contrast in breast diaphanography*", Sima Ertefai et al., Med. Phys. 12 (4), Jul./Aug. 1985, 1985 Am. Assoc. Phys. Med.

"*Optical properties of human dermis in vitro and in vivo*", R. Graaff et al., Feb. 1, 1993 / vol. 32, No. 4 / Applied Optics.

"*Mie and Rayleigh modeling of visible–light scattering in neonatal skin*", Iyad S. Saidi et al., Applied Optics /vol. 34, No. 31 / Nov. 1, 1995.

"*Diffuse reflectance from a finite blood medium: applications to the modeling of fiber optic catheters*", Larry Reynolds et al., Sep. 1976 / vol. 15, No. 9 / Applied Optics.

"*Pulse oximetry: Historical review and Ohmeda functional analysis*", Michael W. Wukitsch, International Journal of Clinical Monitoring and Computing 4: 161–166, 1987.

"*Effect of Anemia on Pulse Oximeter Accuracy at Low Saturation*", John W. Everinghaus, MD et al., Journal of Clinical Monitoring vol. 6, No. 2, Apr. 1990.

"*Design and Evaluation of a New Reflectance Pulse Oximeter Sensor*", Y. Mendelson, Ph.D. et al., Medical Instrumentation vol. 22, No. 4, Aug. 1988.

"*Errors in 14 Pulse Oximeters During Profound Hypoxia*", John W. Severinghaus, MD et al., Journal of Clinical Monitoring, vol. 5, No. 2, Apr. 1989.

"*Accuracy of Response of Six Pulse Oximeters to Profound Hypoxia*", John W. Severinghaus MD et al., Anesthesiology, vol. 67, No. 4, Oct. 1987.

"*The influence of changes in blood flow on the accuracy of pulse oximetry in humans*", M. Vegfors et al., Acta Anaesthesial Scand. 1992: 36: 346–349.

"*Evaluation of Light–Emitting Diodes for Whole Blood Oximetry*", A.P. Shepherd et al., IEEE Transactions on Biomedical Engineering, vol. BME–31, No. 11, Nov. 1984.

"*Noninvasive Methods for Estimating In Vivo Oxygenation*", David A. Benaron, MD et al.,Clinical Pediatrics, May 1992.

"*In Vivo Reflectance of Blood and Tissue as a Function of Light Wavelength*", Weijia Cui et al., IEEE Transactions on Biomedical Engineering, vol. 37, No. 6, Jun. 1990.

"*A Non–Invasive Reflectance Oximeter as a Useful Monitor in ICU*", Y. Shimada et al., Anesthesiology, V. 71, No. 3A, Sep. 1989.

"*Experimental and Clinical Evaluations of a Noninvasive Reflectance Pulse Oximeter Sensor*", Setsuo Takatani et al., Journal of Clinical Monitoring, vol. 8, No. 4, Oct. 1992.

"*Fetal monitoring by pulse oximetry and CTG*", Helen McNamara et al., McNamara & Johnson, Fetal pulse oximetry, J. Perinat. Med. 21 (1993).

"*Noninvasive measurement of regional cerebrovascular oxygen saturation in humans using optical spectroscopy*", Patrick W. McCormick et al., SPIE vol. 1431 Time–Resolved Spectroscopy and Imaging of Tissues (1991).

"*Statistic of penetration depth of photons re–emitted from irradiated tissue*", George H. Weiss et al., Journal of Modern Optics, 1989, vol. 36, No. 3, 349–359.

"*Intrapartum fetal pulse oximetry: Fetal oxygen saturation trends during labor and relation to delivery outcome*", Gary A. Dildy, MD et al., Sep. 1994, Am. J. Obstet. Gynecol.

"*Fetal Oxygenation in Chronic Maternal Hypoxia: What's Critical?*", Berend Oeseburg et al., *Oxygen Transport to Tissue XIV*, Edited by W. Erdmann et al., Plenum Press, New York 1992.

"*Electrocortical activity, electroocular activity, and breathing movements in fetal sheep with prolonged and graded hypoxemia*", Bryan S. Richardson MD et al., Aug. 1992, Am J Obstet Gynecol.

"*Model for photon migration in turbid biological media*", R.F. Bonner et al., 1987 Optical Society of America.

"*Simple Photon Diffusion Analysis of the Effects of Multiple Scattering on Pulse Oximetry*", Joseph M. Schmitt, IEEE Transactions on Biomedical Engineering, vol. 38, No. 12, Dec. 1991.

"*Absorption Spectra of Human Fetal and Adult Oxyhemoglobin, De–Oxyhemoglobin, Carboxyhemoglobin, and Methemoglobin*", W.G. Zijlstra et al., Clinical Chemistry, vol. 37, No. 9, 1991.

"*Reflectance Pulse Oximetry (RPOX): Two Sensors Compared in Piglets*", Roel Niiland et al., Am J Obstat Gynecol, Jan. 1995, vol. 172, No. 1, Part 2.

"*Time resolved reflectance and transmittance for the noninvasive measurement of tissue optical properties*", Michael S. Patterson et al., Applied Optics, Jun. 15, 1989 / vol. 28, No. 12.

"*Tissue Optics Applied to Reflectance Pulse Oximetry*", Reindert Graaff, 1993.

"*Reflectance Pulse Oximetry in Fetal Lambs*", A. Carin Dassel et al., 11264 Pediatric Research, 31 (1992) Mar., No. 3, Baltimore, U.S., vol. 31, No. 3, 1992.

* cited by examiner

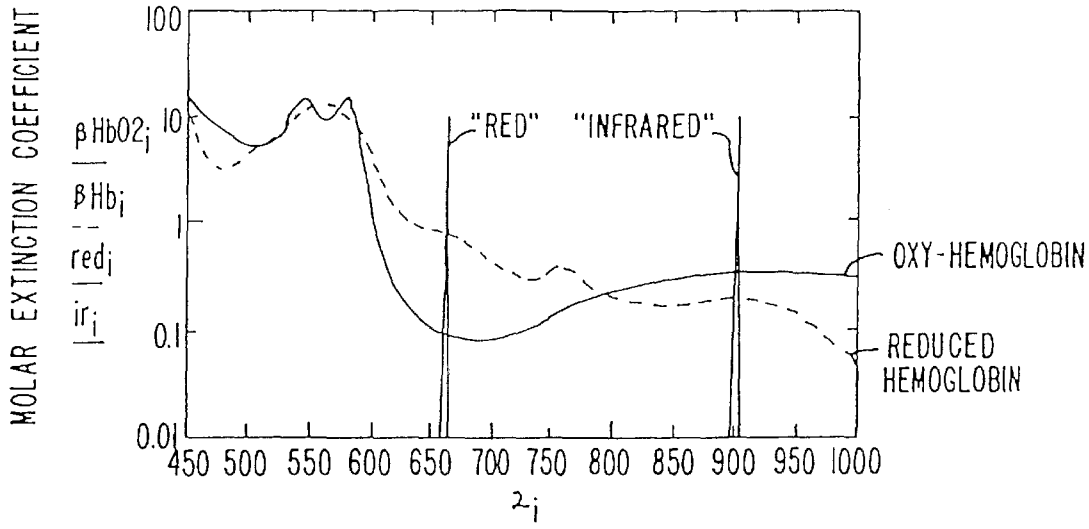

FIG. 1.

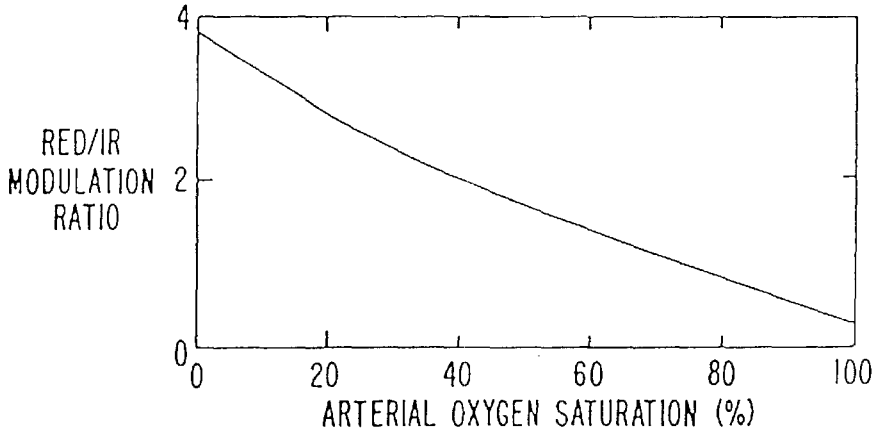

FIG. 2.

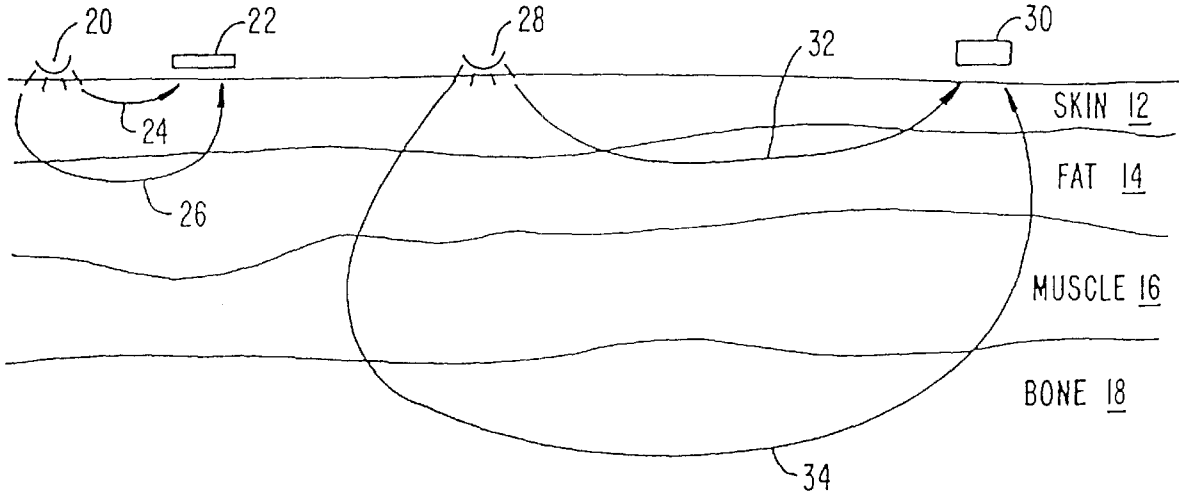

FIG. 3.

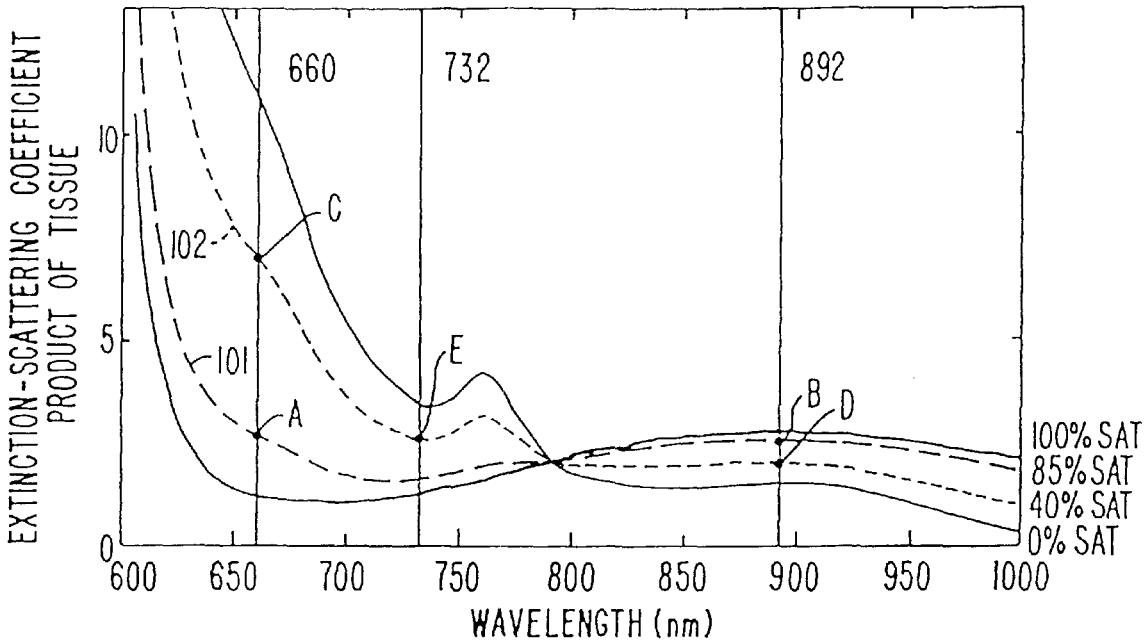

FIG. 4A.

EXTINCTION-SCATTERING COEFFICIENT PRODUCT	660 nm	732 nm	892 nm
(L/mmole-cm^2)			
$\mu'_s \cdot \beta_{HbO2}$	1.23	1.31	2.82
$\mu'_s \cdot \beta_{85\%}$	2.67	1.63	2.64
$\mu'_s \cdot \beta_{40\%}$	7.00	2.58	1.84
$\mu'_s \cdot \beta_{Hb}$	10.85	3.41	1.59

FIG. 4B.

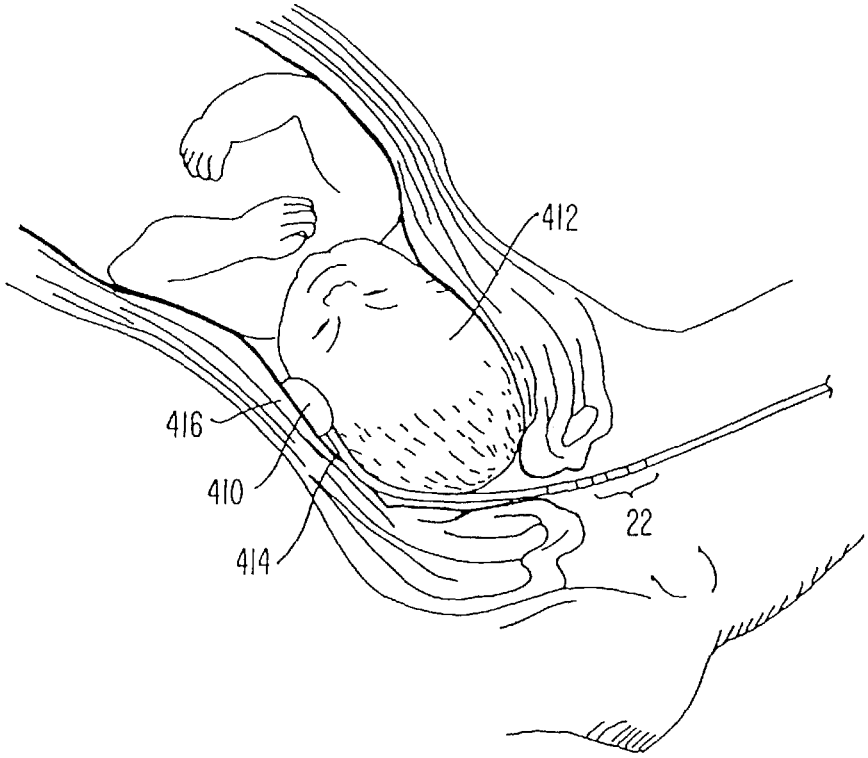

FIG. 5.

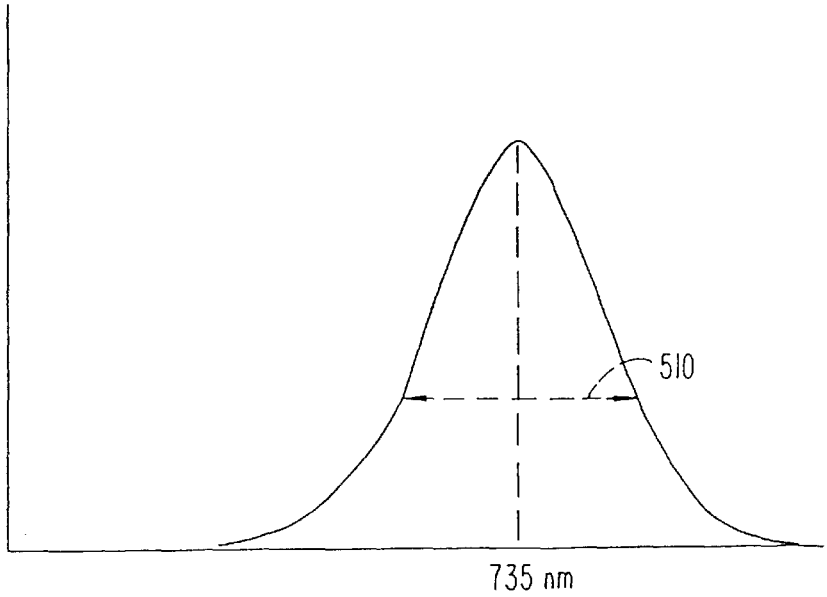

FIG. 6.

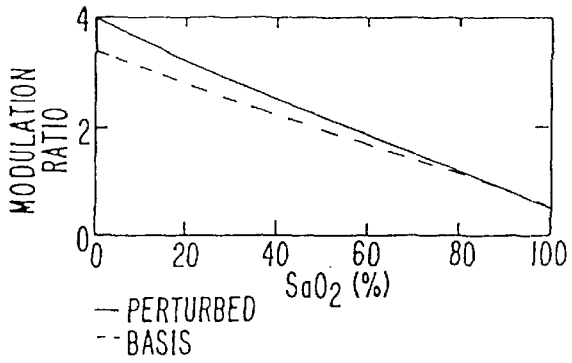

FIG. 7A.

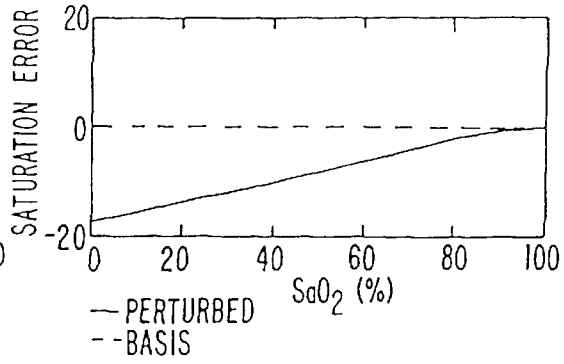

FIG. 7B.

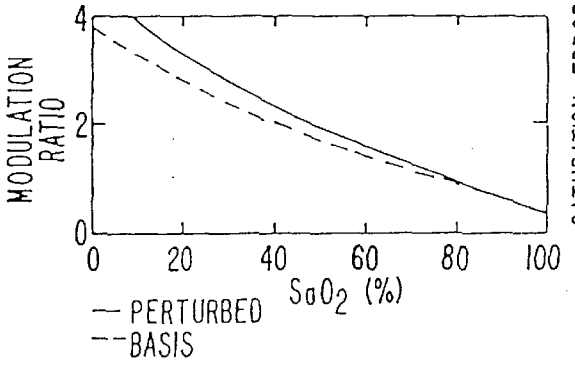

FIG. 8A.

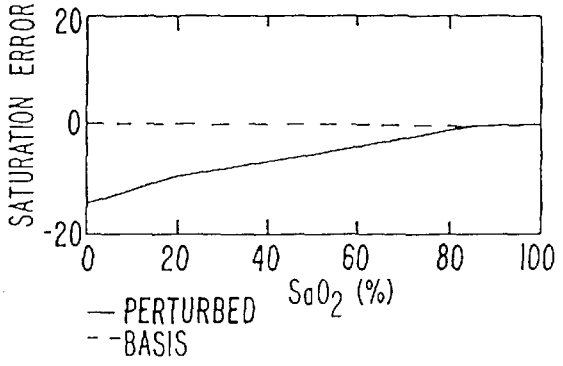

FIG. 8B.

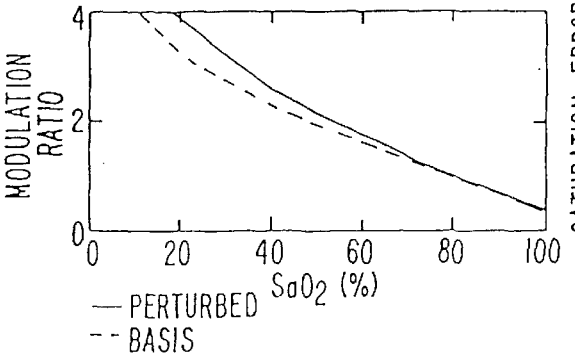

FIG. 9A.

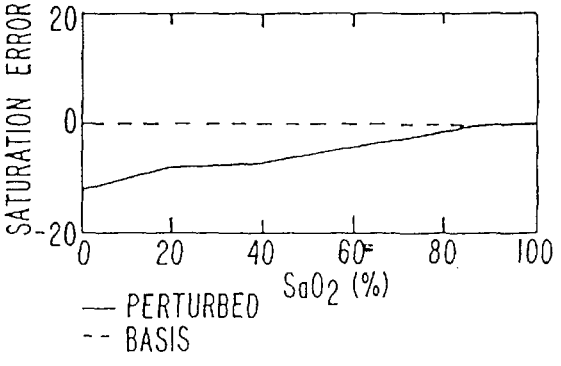

FIG. 9B.

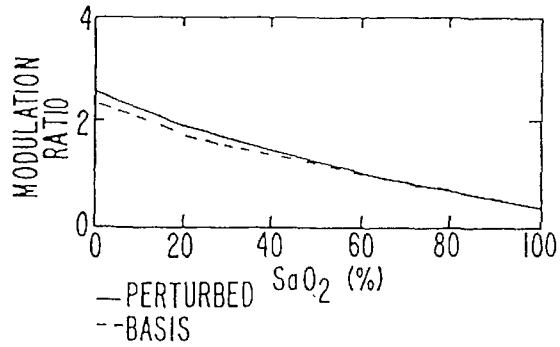

FIG. 10A.

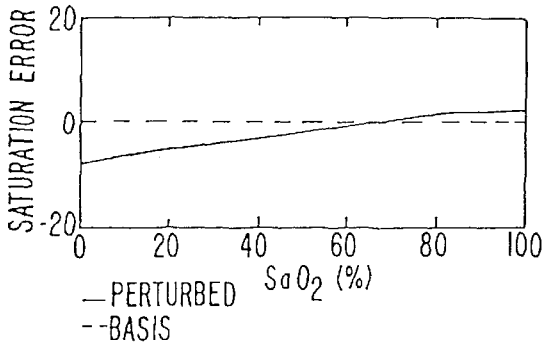

FIG. 10B.

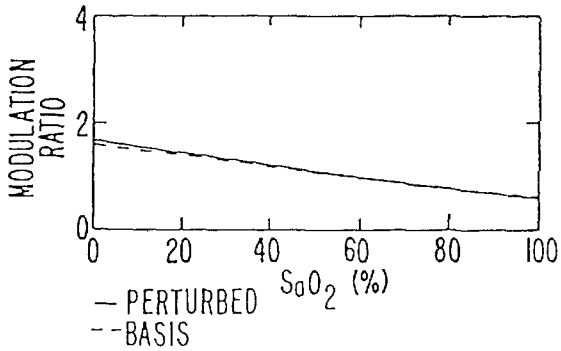

FIG. 11A.

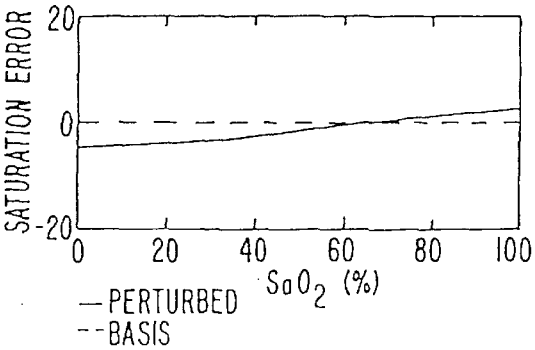

FIG. 11B.

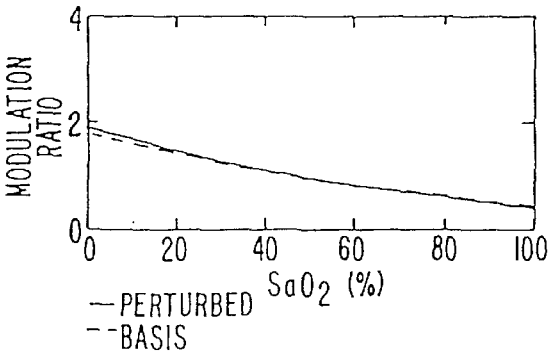

FIG. 12A.

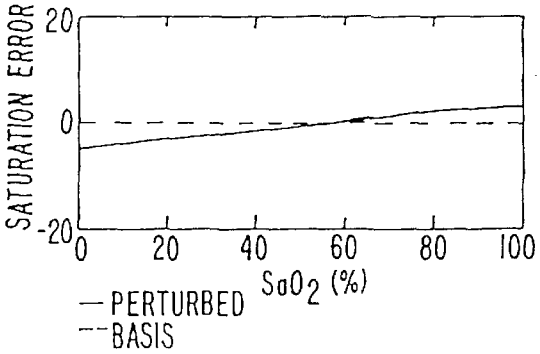

FIG. 12B.

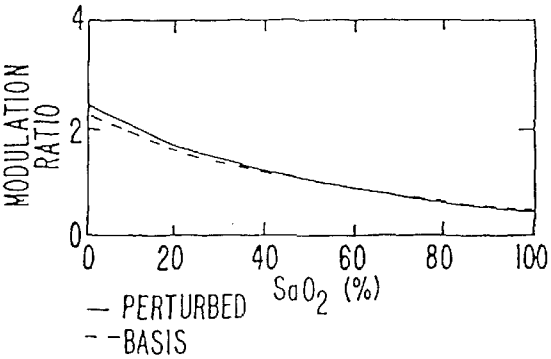

FIG. 13A.

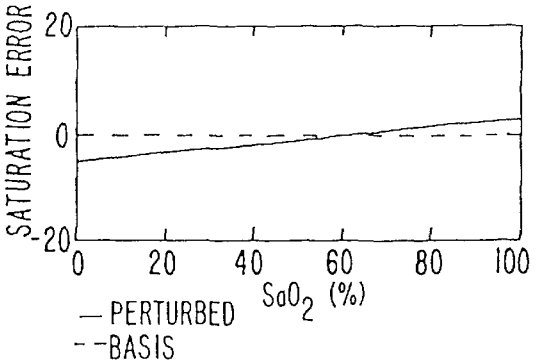

FIG. 13B.

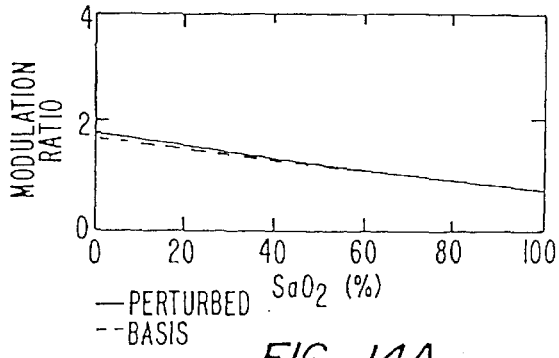

FIG. 14A.

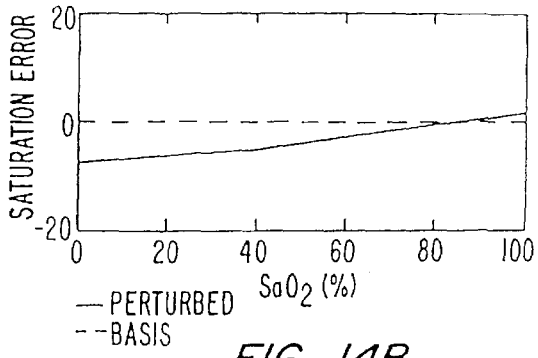

FIG. 14B.

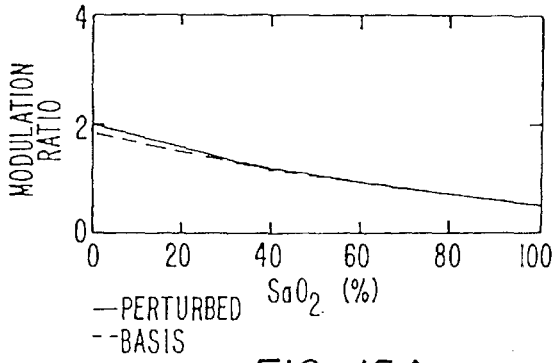

FIG. 15A.

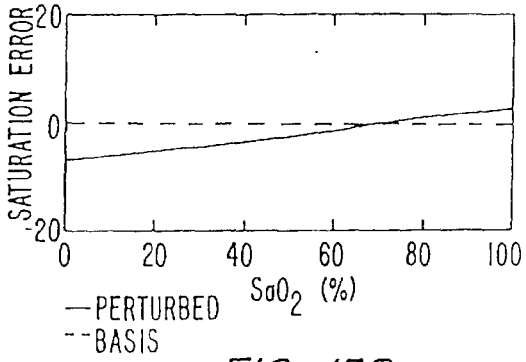

FIG. 15B.

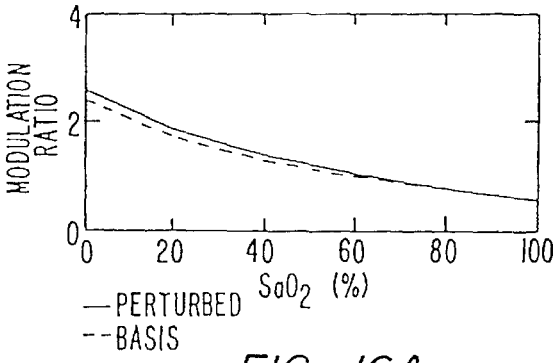

FIG. 16A.

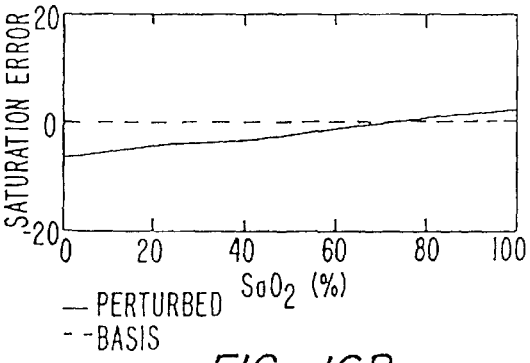

FIG. 16B.

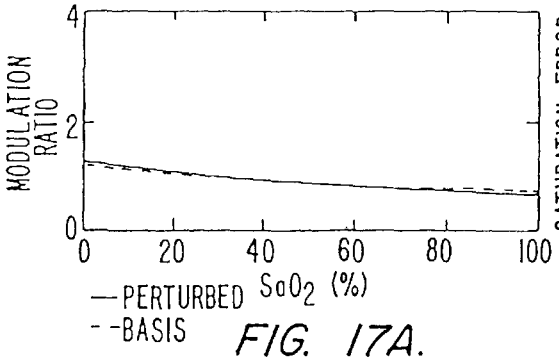

FIG. 17A.

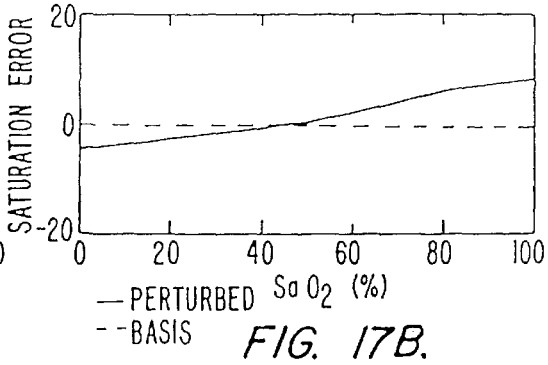

FIG. 17B.

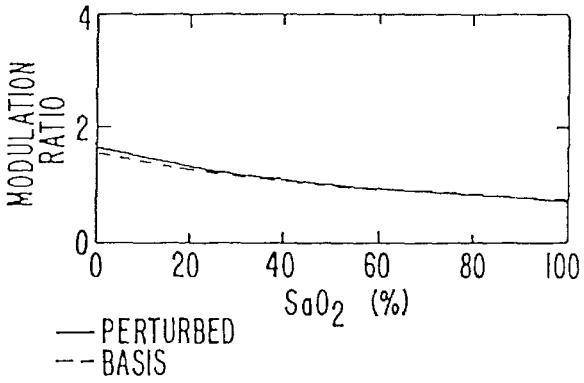

FIG. 18A.

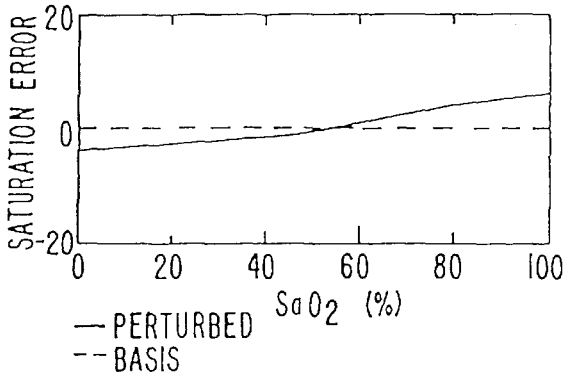

FIG. 18B.

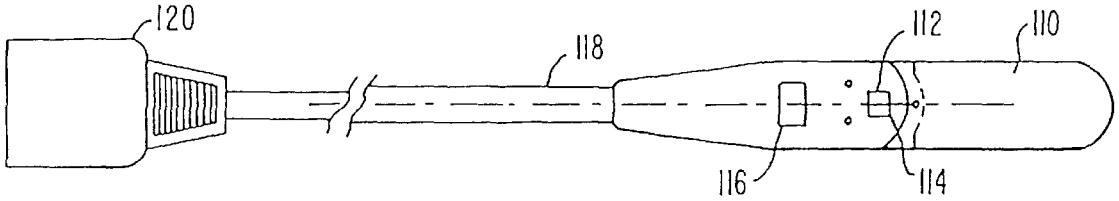

FIG. 24.

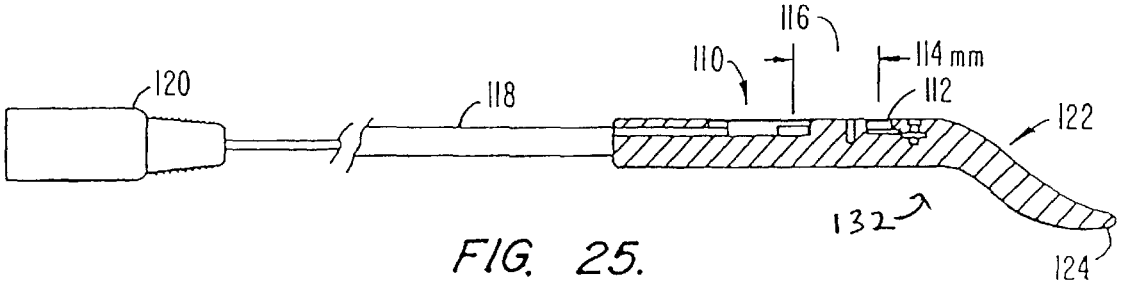

FIG. 25.

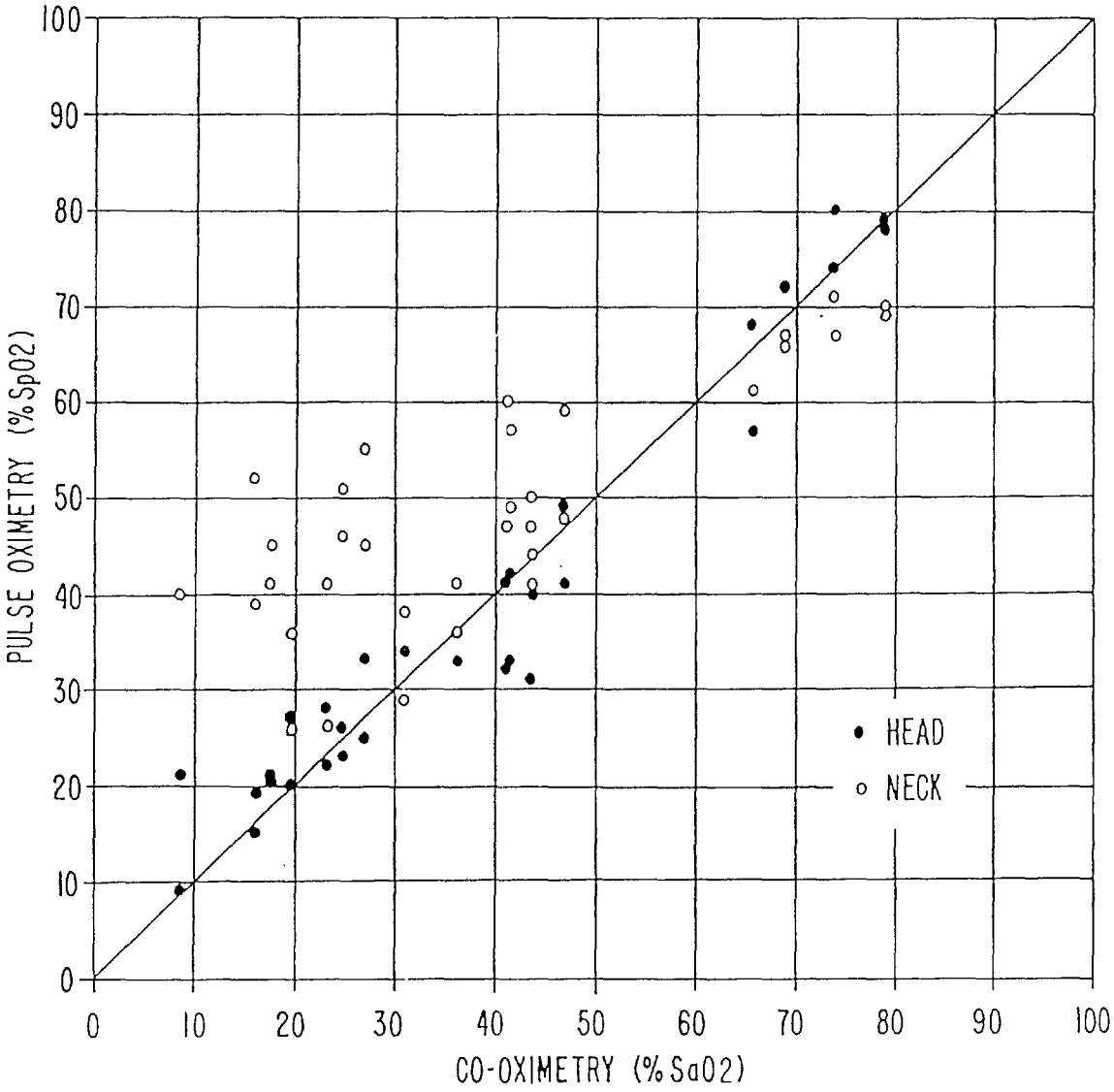
PULSE OXIMETRY (%SpO2)
CO-OXIMETRY (%SaO2)
0
10
20
30
40
50
60
70
80
90
100
HEAD
NECK

FIG. 19.

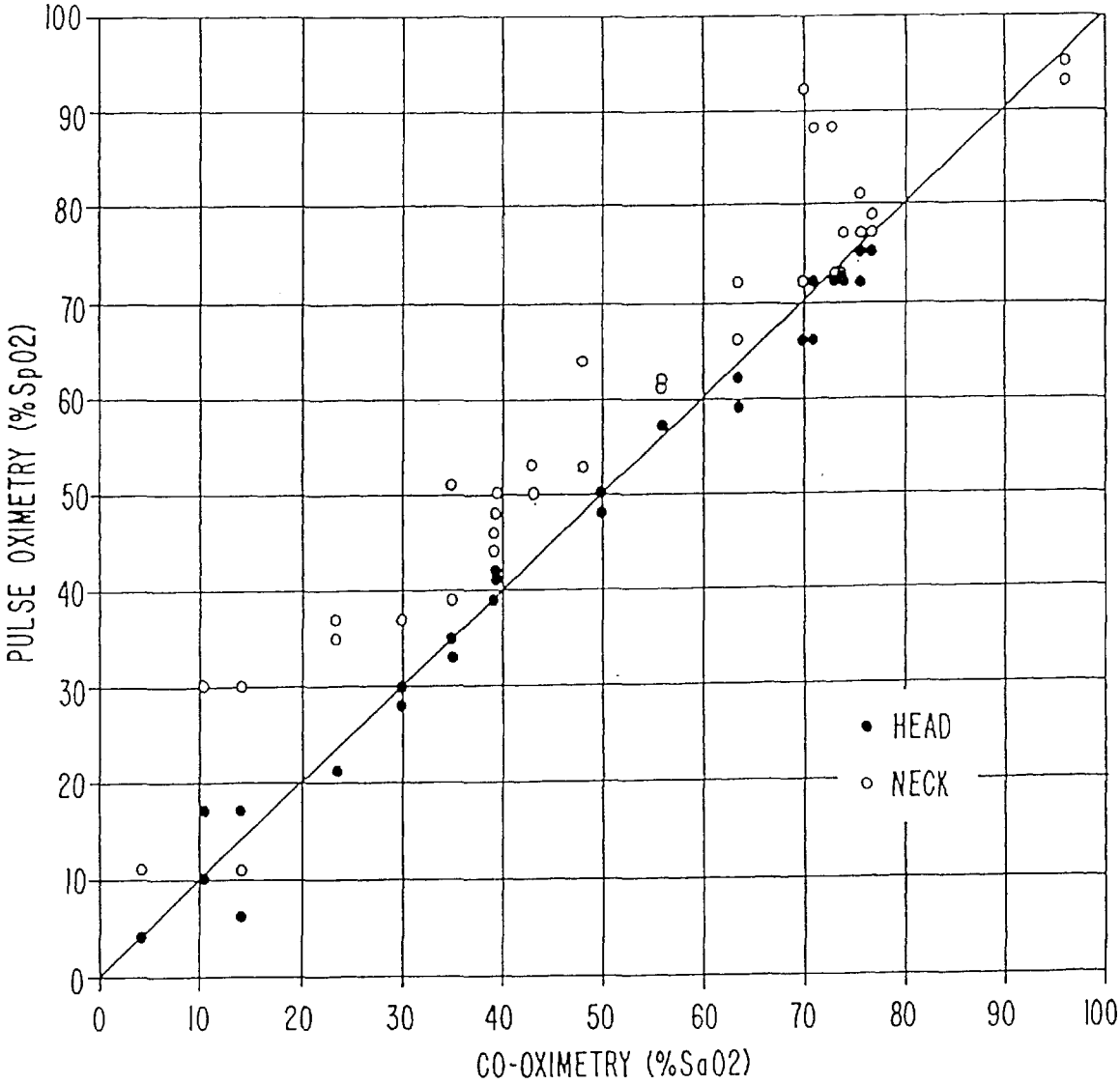
PULSE OXIMETRY (%SpO2)
CO-OXIMETRY (%SaO2)
0
10
20
30
40
50
60
70
80
90
100
HEAD
NECK

FIG. 20.

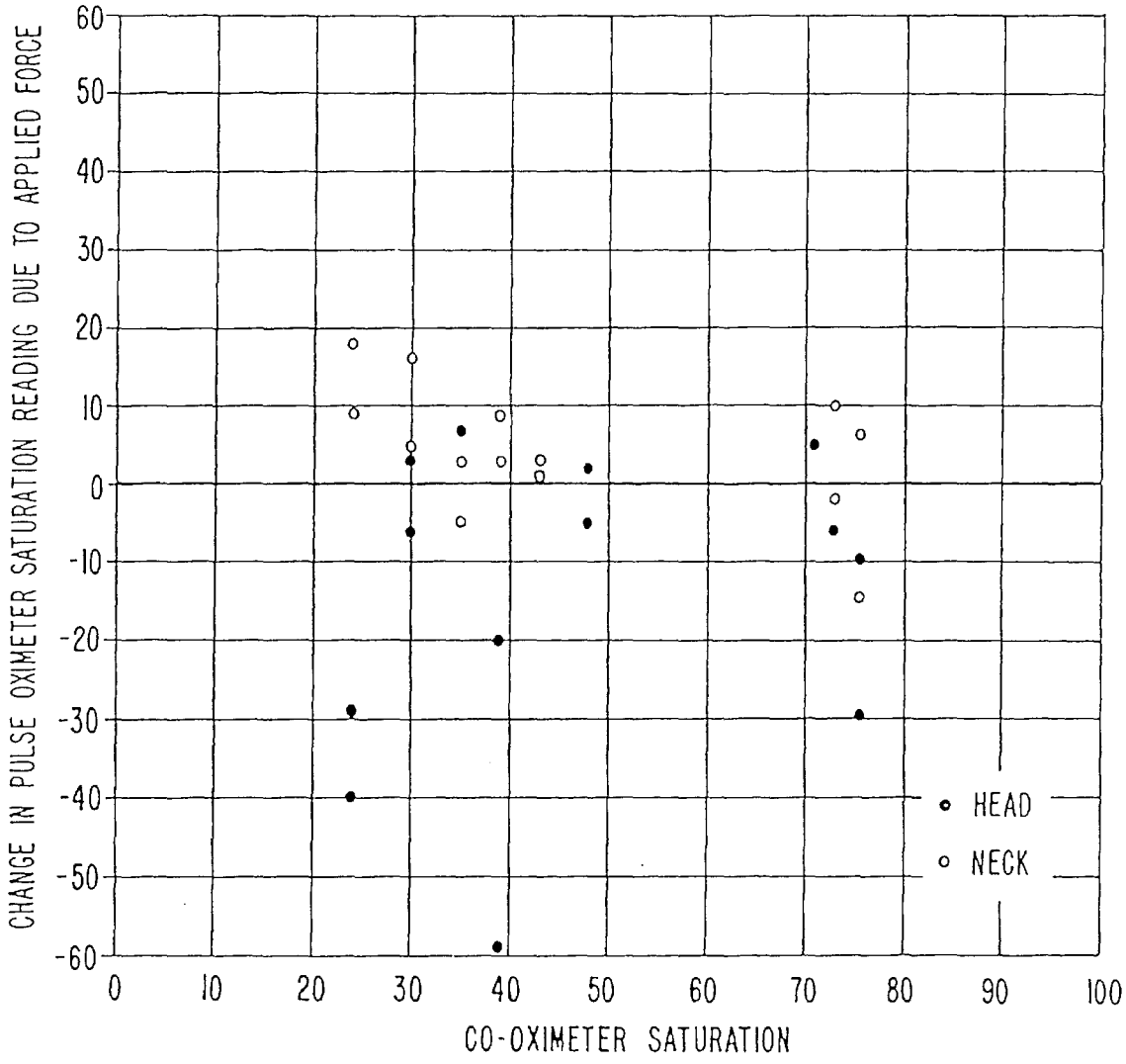
CHANGE IN PULSE OXIMETER SATURATION READING DUE TO APPLIED FORCE
60
50
40
30
20
10
0
-10
-20
-30
-40
-50
-60
0
10
20
30
40
50
60
70
80
90
100
CO-OXIMETER SATURATION
HEAD
NECK

FIG. 21.

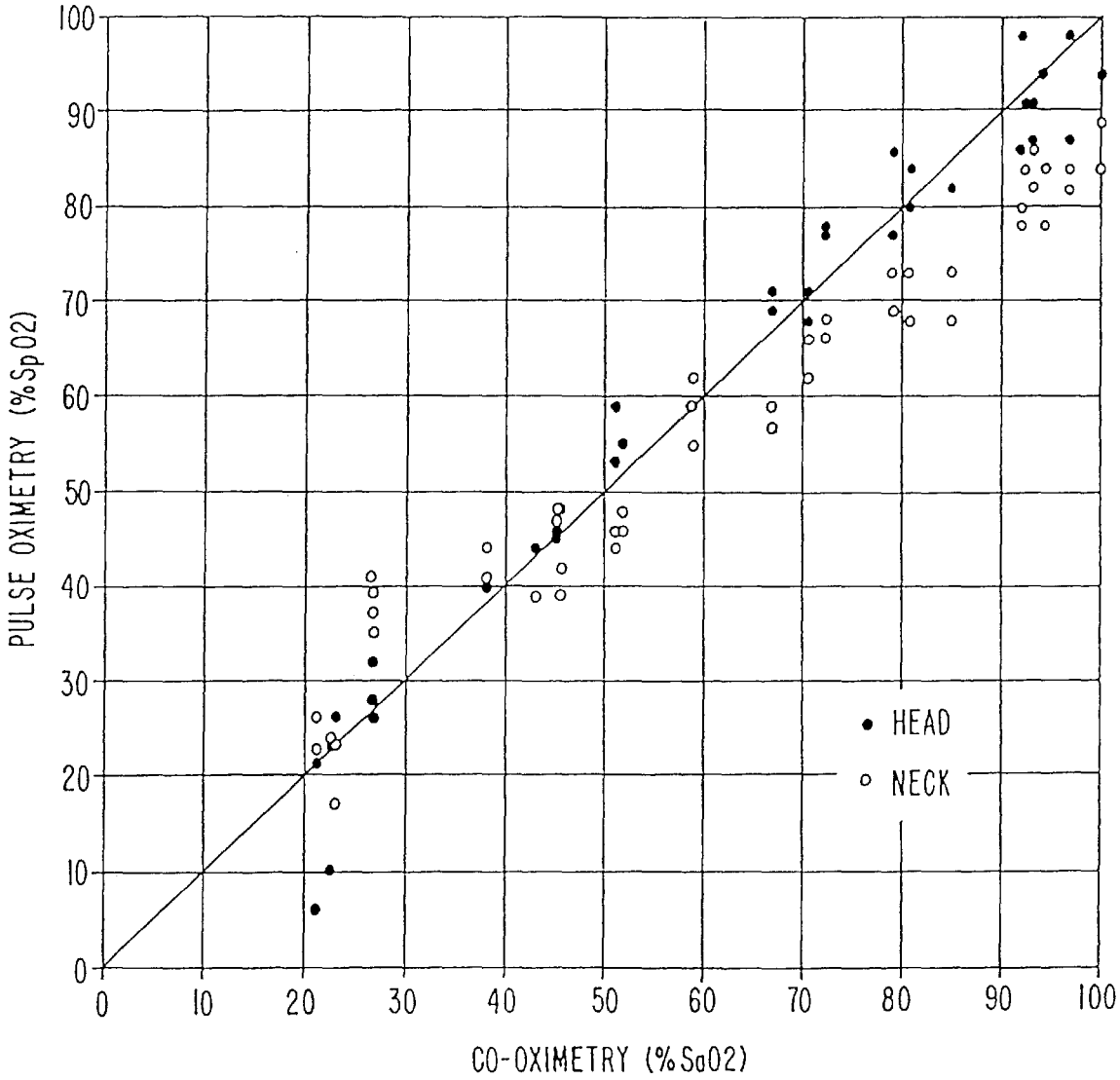
PULSE OXIMETRY (%SpO2)
CO-OXIMETRY (%SaO2)
0
10
20
30
40
50
60
70
80
90
100
HEAD
NECK

FIG. 22.

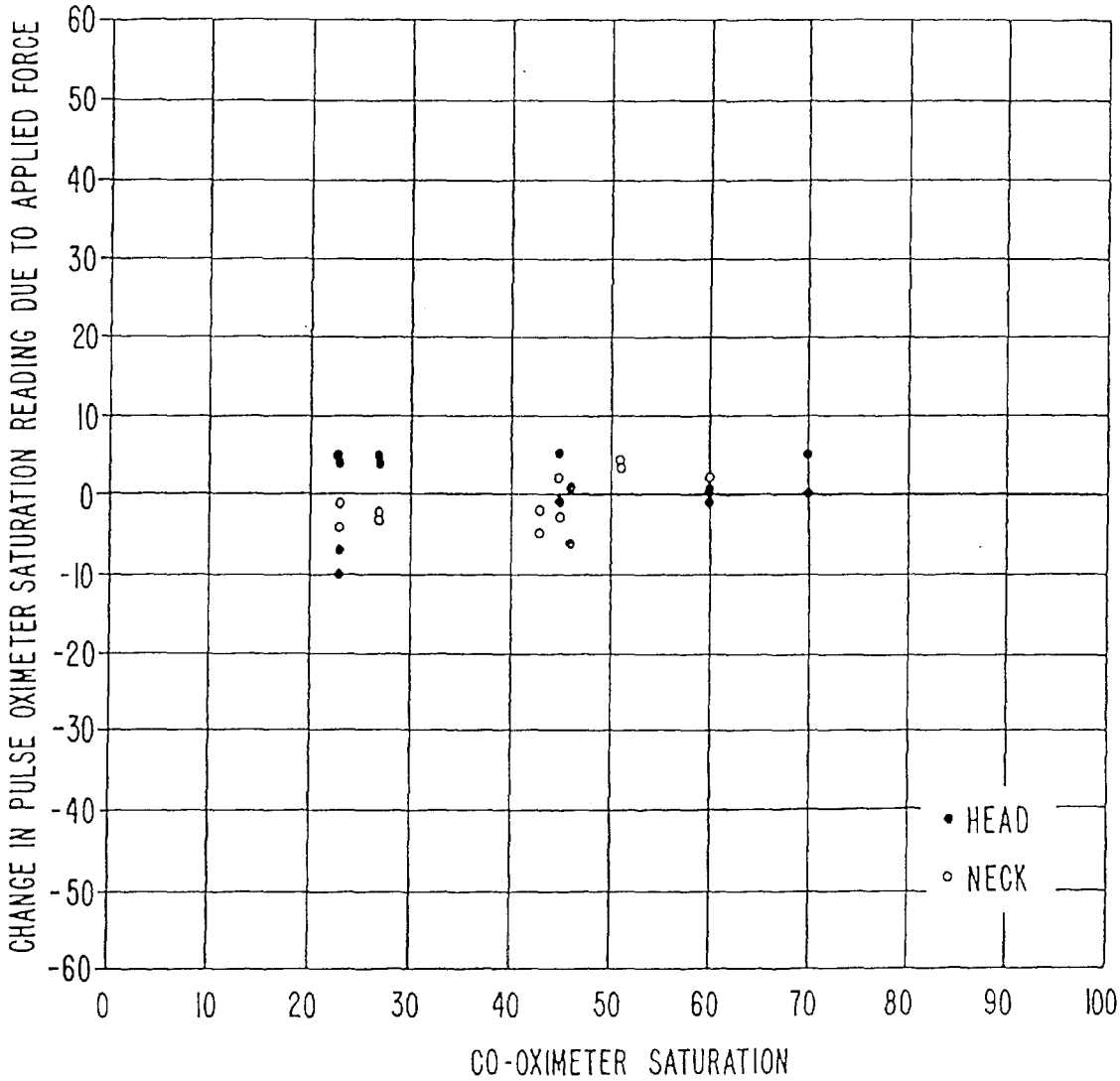
CHANGE IN PULSE OXIMETER SATURATION READING DUE TO APPLIED FORCE
60
50
40
30
20
10
0
-10
-20
-30
-40
-50
-60
0
10
20
30
40
50
60
70
80
90
100
CO-OXIMETER SATURATION
8
8
• HEAD
○ NECK

FIG. 23.

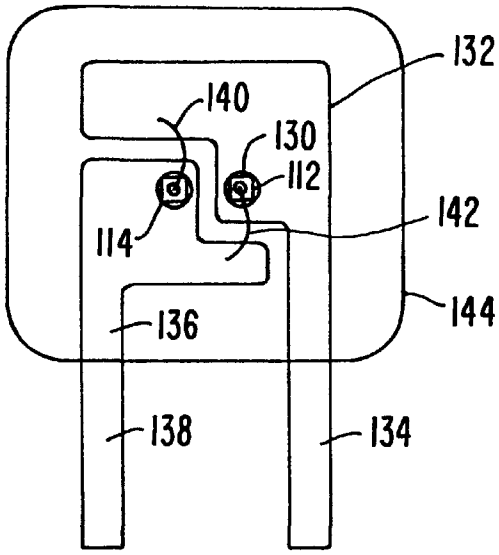

FIG. 26A.

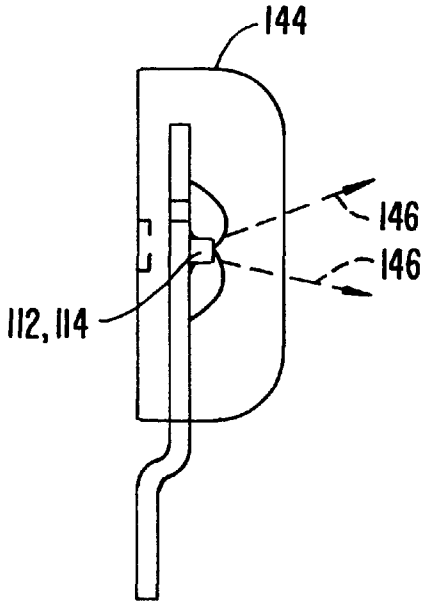

FIG. 26B.

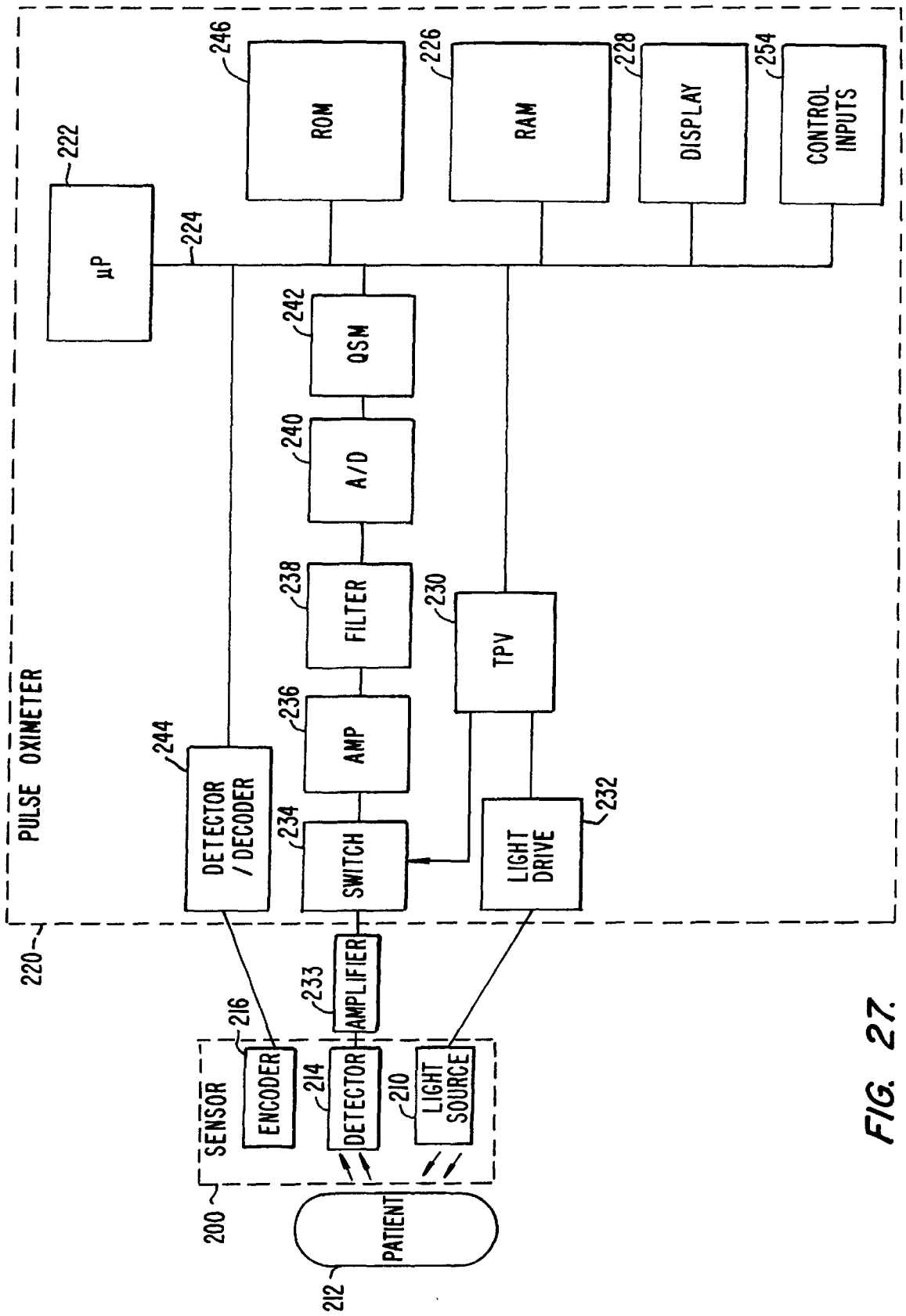
PULSE OXIMETER
220
µP
222
224
ROM
246
RAM
226
DISPLAY
228
CONTROL INPUTS
254
QSM
242
A/D
240
FILTER
238
AMP
236
SWITCH
234
TPV
230
LIGHT DRIVE
232
DETECTOR / DECODER
244
AMPLIFIER
233
SENSOR
200
ENCODER
216
DETECTOR
214
LIGHT SOURCE
210
PATIENT
212

FIG. 27.

PULSE OXIMETER AND SENSOR OPTIMIZED FOR LOW SATURATION

CROSS-REFERENCE TO RELATED APPLICATIONS

This is a continuation of U.S. application Ser. No. 09/003,413, filed Jan. 6, 1998, now U.S. Pat. No. 6,272,363, which is a continuation of U.S. application Ser. No. 08/413,578, filed Mar. 30, 1995, now U.S. Pat. No. 5,782,237, which is a continuation-in-part of U.S. application Ser. No. 08/221,911, filed Apr. 1, 1994, now U.S. Pat. No. 5,421,329, which disclosures are incorporated herein by reference.

BACKGROUND OF THE INVENTION

Pulse oximetry is used to continuously monitor the arterial blood oxygen saturation of adults, pediatrics and neonates in the operating room, recovery room, intensive care units, and increasingly on the general floor. A need exists for pulse oximetry in the delivery room for monitoring the oxygen status of a fetus during labor and delivery, and for monitoring the oxygen status of cardiac patients.

Pulse oximetry has traditionally been used on patient populations where arterial blood oxygen saturation is typically greater than 90%, i.e., more than 90% of the functional hemoglobin in the arterial blood is oxyhemoglobin and less than 10% is reduced hemoglobin. Oxygen saturation in this patient population rarely drops below 70%. When it does drop to such a low value, an unhealthy clinical condition is indicated, and intervention is generally called for. In this situation, a high degree of accuracy in the estimate of saturation is not clinically relevant, as much as is the trend over time.

Conventional two wavelength pulse oximeters emit light from two Light Emitting Diodes (LEDs) into a pulsatile tissue bed and collect the transmitted light with a photodiode positioned on an opposite surface (transmission pulse oximetry), or an adjacent surface (reflectance pulse oximetry). The LEDs and photodetector are housed in a reusable or disposable sensor which connects to the pulse oximeter electronics and display unit. The "pulse" in pulse oximetry comes from the time varying amount of arterial blood in the tissue during the cardiac cycle, and the processed signals from the photodetector create the familiar plethysmographic waveform due to the cycling light attenuation. For estimating oxygen saturation, at least one of the two LEDs' primary wavelength must be chosen at some point in the electromagnetic spectrum where the absorption of oxyhemoglobin (HbO_2) differs from the absorption of reduced hemoglobin (Hb). The second of the two LEDs' wavelength must be at a different point in the spectrum where, additionally, the absorption differences between Hb and HbO_2 are different from those at the first wavelength. Commercial pulse oximeters utilize one wavelength in the near red part of the visible spectrum near 660 nanometers (nm), and one in the near infrared part of the spectrum in the range of 880 nm–940 nm (See FIG. **1**). As used herein, "red" wavelengths or "red" spectrum will refer to the 600–800 nm portion of the electromagnetic spectrum; "near red", the 600–700 nm portion; "far red", the 700–800 nm portion; and "infrared" or "near infrared", the 800–1000 nm portion.

Photocurrents generated within the photodetector are detected and processed for measuring the modulation ratio of the red to infrared signals. This modulation ratio has been observed to correlate well to arterial oxygen saturation as shown in FIG. **2**. Pulse oximeters and pulse oximetry sensors are empirically calibrated by measuring the modulation ratio over a range of in vivo measured arterial oxygen saturations (SaO_2) on a set of patients, healthy volunteers or animals. The observed correlation is used in an inverse manner to estimate saturation (SpO_2) based on the real-time measured value of modulation ratios. (As used herein, SaO_2 refers to the in vivo measured functional saturation, while SpO_2 is the estimated functional saturation using pulse oximetry.)

The choice of emitter wavelengths used in conventional pulse oximeters is based on several factors including, but not limited to, optimum signal transmission through blood perfused tissues, sensitivity to changes in arterial blood oxygen saturation, and the intensity and availability of commercial LEDs at the desired wavelengths. Traditionally, one of the two wavelengths is chosen from a region of the absorption spectra (FIG. **1**) where the extinction coefficient of HbO_2 is markedly different from Hb. The region near 660 nm is where the ratio of light absorption due to reduced hemoglobin to that of oxygenated hemoglobin is greatest. High intensity LEDs in the 660 nm region are also readily available. The IR wavelength is typically chosen near 805 nm (the isosbestic point) for numerical convenience, or in the 880–940 nm spectrum where additional sensitivity can be obtained because of the inverse absorption relationship of Hb and HbO_2. Unfortunately, pulse oximeters which use LED wavelengths paired from the 660 nm band and 900 nm bands all show diminished accuracy at low oxygen saturations.

SUMMARY OF THE INVENTION

According to the invention, more accurate estimates of low arterial oxygen saturation using pulse oximetry are achieved by optimizing a wavelength spectrum of first and second light sources so that the saturation estimates at low saturation values are improved while the saturation estimates at high saturation values are minimally adversely affected as compared to using conventional first and second wavelength spectrums. It has been discovered that calculations at low saturation can be significantly improved if the anticipated or predicted rates of absorption and scattering of the first wavelength spectrum is brought closer to, optimally equal to, the anticipated or predicted rates of absorption and scattering of the second wavelength spectrum than otherwise exists when conventional wavelength spectrum pairs are chosen, such as when conventionally using a first wavelength centered near 660 nm and a second wavelength centered anywhere in the range of 880 nm–940 nm.

The present invention solves a long felt need for a pulse oximeter sensor and system which provides more accurate estimates of arterial oxygen saturation at low oxygen saturations, i.e. saturations equal to or less than 80%, 75%, 70%, 65%, or 60%, than has heretofore existed in the prior art. The sensor and system is particularly useful for estimating arterial saturation of a living fetus during labor where the saturation range of principal importance and interest is generally between 15% and 65%, and is particularly useful for estimating arterial saturation of living cardiac patients who experience significant shunting of venous blood into their arteries in their hearts and hence whose saturation range of principle importance and interest is roughly between 50% and 80%. By contrast, a typical healthy human has a saturation greater than 90%. The invention has utility whenever the saturation range of interest of a living subject, either human or animal, is low.

In addition to providing better estimates of arterial oxygen saturation at low saturations, the sensor, monitor, and system

of the invention further provide better and more accurate oxygen saturation estimates when perturbation induced artifacts exist and are associated with the subject being monitored.

When the rates of absorption and scattering by the tissue being probed by the first and second wavelength spectrums are brought closer together for the saturation values of particular interest, improved correspondence and matching of the tissue actually being probed by the first and second wavelengths is achieved, thus drastically reducing errors introduced due to perturbation induced artifacts. For example, when light of one wavelength is absorbed at a rate significantly higher than that of the other wavelength, the light of the other wavelength penetrates significantly further into the tissue. When the tissue being probed is particularly in-homogenous, this difference in penetrations can have a significant adverse impact on the accuracy of the arterial oxygen saturation estimate.

Perturbation induced artifacts include, but are not limited to, any artifact that has a measurable impact on the relative optical properties of the medium being probed.

Perturbation induced artifacts include but are not limited to the following:

(1) variations in the tissue composition being probed by the sensor from subject to subject, i.e., variations in the relative amounts of fat, bone, brain, skin, muscle, arteries, veins, etc.;

(2) variations in the hemoglobin concentration in the tissue being probed, for example caused by vasal dilations or vasal constrictions, and any other physical cause which affects blood perfusion in the tissue being probed; and

(3) variations in the amount of force applied between the sensor and the tissue being probed, thus affecting the amount of blood present in the nearby tissue.

In one embodiment, the present invention provides a fetal pulse oximeter sensor with a light source optimized for the fetal oxygen saturation range and for maximizing the immunity to perturbation induced artifact. Preferably, a far red and an infrared light source are used, with the far red light source having a mean wavelength between 700–790 nm. The infrared light source can have a mean wavelength as in prior art devices used on patients with high saturation, i.e., between 800–1000 nm. As used herein, "high saturation" shall mean an arterial oxygen saturation greater than 70%, preferably greater than 75%, alternatively greater than 80%, optionally greater than 90%.

The fetal sensor of the present invention is further optimized by arranging the spacing between the location the emitted light enters the tissue and the location the detected light exits the tissue to minimize the sensitivity to perturbation induced artifact.

According to a preferred embodiment, electrooptic transducers (e.g., LEDs and photodetectors) are located adjacent to the tissue where the light enters and exits the tissue. According to an alternate embodiment, the optoelectric transducers are located remote from the tissue, for example in the oximeter monitor, and optical fibers interconnect the transducers and the tissue with the tissue being illuminated from an end of a fiber, and light scattered by the tissue being collected by an end of a fiber. Multiple fibers or fiber bundles are preferred.

The present invention recognizes that the typical oxygen saturation value for a fetus is in the range of 5–65%, commonly 15–65%, compared to the 90% and above for a typical patient with normal (high) saturation. In addition, a fetal sensor is subject to increased perturbation induced artifact. Another unique factor in fetal oximetry is that the sensor is typically inserted through the vagina and the precise location where it lands is not known in advance.

The present invention recognizes all of these features unique to fetal oximetry or oximetry for low saturation patients and provides a sensor which optimizes the immunity to perturbation induced artifacts. This optimization is done with a trade-off on the sensitivity to changes in saturation value. This trade-off results in a more reliable calculation that is not obvious to those who practice the prior art methods which attempt to maximize the sensitivity to changes in the saturation value. The improvement in performance that results from these optimizations are applicable to both reflectance and transmission pulse oximetry. An example of a fetal transmission pulse oximetry configuration usable with the present invention is described in U.S. patent application Ser. No. 07/752,168, assigned to the assignee of the present invention, the disclosure of which is incorporated herein by reference. An example of a non-fetal transmission pulse oximetry configuration usable with the present invention is described in U.S. Pat. No. 4,830,014, assigned to the assignee of the present invention, the disclosure of which is incorporated herein by reference.

BRIEF DESCRIPTION OF THE DRAWINGS

FIG. **1** is a chart of the absorption characteristics of oxyhemoglobin (HbO_2) and reduced hemoglobin (Hb) versus wavelength showing prior art near red and infrared LED wavelengths;

FIG. **2** is a graph of red/IR modulation ratio versus oxygen saturation;

FIG. **3** is a diagram illustrating light penetration through different layers of tissue at different distances;

FIG. **4**A is a chart of the variation in extinction and scattering coefficients over a range of wavelengths for different saturation values;

FIG. **4**B is a table of the values of FIG. **4**A;

FIG. **5** is a diagram illustrating the placing of a sensor on a fetus;

FIG. **6** is a graph illustrating the spectrum of an LED according to the present invention;

FIGS. **7–18** are graphs showing experimental modeling of the modulation ratio and saturation error as a function of saturation for different red and infrared wavelength combinations;

FIGS. **19–23** are charts illustrating saturation and the error due to applied force for different combinations of emitter wavelength and emitter-detector spacing from experiments done on sheep;

FIGS. **24** and **25** are diagrams illustrating the construction of a sensor according to the present invention;

FIGS. **26**A–B are diagrams of a single package, dual emitter package used in the present invention; and

FIG. **27** is a block diagram of a pulse oximeter according to the present invention.

DETAILED DESCRIPTION OF THE PREFERRED EMBODIMENTS

An understanding of the design of the fetal sensor according to the present invention requires an understanding of the environment in which the sensor will operate. FIG. **3** illustrates the layers of tissue in a typical fetus location where a sensor may be applied. Typically, there would be a first layer

of skin **12**, perhaps followed by a layer of fat **14**, a layer of muscle **16**, and a layer of bone **18**. This is a simplified view for illustration purposes only. The contours and layers can vary at different locations. For instance, bone would be closer to the surface on the forehead, as opposed to closer muscle on the neck. Such variations in sites can produce the first type of perturbation artifact mentioned in the summary—artifact due to variations in tissue composition.

The general paths of light from an emitter **20** to a photodetector **22** are illustrated by arrows **24** and **26**. Arrow **24** shows light which passes almost directly from emitter **20** to detector **22**, basically shunted from one to the other, passing through very little blood perfused tissue. Arrow **26**, on the other hand, illustrates the deeper penetration of another path of the light. The depth of penetration is affected by the wavelength of the light and the saturation. At low saturation, infrared light penetrates deeper than near red, for instance. The deeper penetration can result in an undesirable variation between the infrared and red signals, since the IR signal will pass through more different layers.

Also illustrated in FIG. **3** is the effect of using an emitter **28** which is spaced on the tissue at a greater distance from a detector **30** than the first pair **20**, **22** described. As can be seen, this greater separation results in the penetration of a larger amount of tissue, as indicated by arrows **32** and **34**. Thus, the greater spacing increases the depth of penetration, although it will reduce the intensity of the signal received at the detector due to more attenuation from more of the light being absorbed in the tissue and the greater light propagation distances involved.

The second type of perturbation mentioned in the summary is variations in the concentration of blood in the tissue from patient to patient or over time. A lower concentration results in less absorption, increasing the penetration depth. The inventors estimate that the mean penetration depth of photons in a medium is related to the product of the absorption and scattering coefficients, and this estimate is consistent with the findings of Weiss et al., *Statistics of Penetration Depth of Photons Re-emitted from Irradiated Tissue,* Journal of Modern Optics, 1989, vol. 36, No. 3, 349–359, 354, the disclosure of which is incorporated herein by reference.

Absorption of light in tissue in the visible and near infrared region of the electromagnetic spectrum is dominated by the absorption characteristics of hemoglobin. Absorption coefficients of hemoglobin can be found in the literature, for example Zijlstra, et al., "Absorption spectra of human fetal and adult oxyhemoglobin, de-oxyhemoglobin, carboxyhemoglobin and methemoglobin", *Clinical Chemistry,* 37/9, 1633–1638, 1991 (incorporated herein by reference). Measured scattering coefficients of tissue are influenced by the methodology of measurement and the model used to fit the data, although there is general agreement in the relative sensitivity to wavelength regardless of method. Tissue scattering coefficients used by the inventors are based on diffusion theory, and are taken from Schmitt, "Simple photon diffusion analysis of the effects of multiple scattering on pulse oximetry", *IEEE Transactions on Biomedical Engineering,* Vol. 38, No. 12, December 1991, the disclosure of which is incorporated herein by reference.

FIG. **4**A is a graph showing the product of the absorption and scattering coefficients for 0%, 40%, 85% and 100% saturations for wavelengths between 600 nm and 1,000 nm. For 85–100% tissue oxygen saturation, good balance or correlation exists between the product of the absorption and scattering coefficients of conventionally chosen wavelength pairs (i.e., 660 nm and 892 nm), as illustrated by points A and B on curve **101**.

For low tissue oxygen saturation, points C and D on curve **102** graphically indicate that there is a very significant mismatch between the product of the absorption and scattering coefficients of the 660 nm near red and 892 nm infrared light, with the near red light being more strongly absorbed and scattered. This very significant absorption and scattering mismatch results in very different tissue being probed by the near red and infrared light which significantly degrades the accuracy of the arterial oxygen saturation calculation. In addition, when a large range of low arterial oxygen saturations need to be accurately calculated, as when monitoring a fetus during labor where the range of arterial oxygen saturations can extend between 15% and 65%, it is evident from FIG. **4**A that not only does a significant mismatch between the rates of absorption and scattering of the near red and infrared light exist, but that the amount of mismatch will vary significantly as arterial oxygen saturation varies, thus causing a differential inaccuracy of oxygen saturation estimates which varies with the arterial saturation.

On the other hand, points D and E on curve **102** in FIG. **4**A illustrate advantages of a preferred embodiment of the invention of choosing first and second wavelengths, i.e., 732 nm and 892 nm, which have absorption and scattering characteristics which are more closely balanced as compared to the prior art pairing of 660 nm and 892 nm for 40% tissue oxygen saturation. As can be appreciated, since the 732 nm extinction and scattering coefficients more nearly match the 892 nm extinction and scattering coefficients, improved overlap of the tissue being probed by the two wavelengths of light result. In addition, 732 nm results in a smaller variation of the extinction and scattering coefficients as a function of oxygen saturation as compared to 660 nm, thus resulting in better and more accurate oxygen saturation estimates over a wider range of saturations. The tissue oxygen saturation values shown in FIG. **4**A are closely correlated to arterial oxygen saturation values. In general, a given value of tissue oxygen saturation corresponds to a higher value of arterial oxygen saturation. For example, the inventors estimate that 85% tissue oxygen saturation corresponds to roughly 100% arterial oxygen saturation.

A preferred embodiment of the invention is to optimize the wavelengths used for a sensor to estimate fetal arterial oxygen saturation during labor where the saturation of interest is below 70%, a typical range of interest being between 15% and 65%. Attempting to match or balance the rates of absorption and scattering of the two wavelengths in a fetal sensor is particularly useful since the amount of perturbation induced artifacts are so severe in number and magnitude. For example, for a surface reflection sensor, it is difficult to know a priori where on the fetus the sensor will be located. For example, sometimes it will be on the head, other times the cheek. Hence, the tissue composition varies from application to application. In addition, the force by which the sensor is applied will vary during labor thus introducing still additional perturbation induced artifacts.

Another preferred embodiment of the invention is to use the sensor of the invention for cardiac patients whose range of saturation, where accuracy in calculations is important, is from 50% to 80%.

FIG. **5** illustrates the placement of a sensor **410** on a fetus **412**. The sensor is connected by a cable **414** to an external pulse oximeter monitor. As can be seen, sensor **410** is wedged between a uterine wall **416** and the fetus **412**. In this instance, the sensor is on the side of the fetus' forehead. This

wedging of the sensor applies a force to the skin immediately below the sensor, which reduces the amount of blood in the local tissue. This reduces the amount of blood the light signal will pass through, thus increasing the difficulty of obtaining an accurate blood oxygenation reading.

In choosing an optimum LED wavelength, it must be kept in mind that LEDs have a spectral width, and are not a single narrowband wavelength device like a laser. FIG. **6** illustrates the spectral spread of one preferred wavelength for a sensor according to the present invention, showing the far red wavelength at 735 nm as being the peak wavelength. However, arrow **510** indicates a distribution of wavelengths which can be approximately 25 nm wide at which the intensity level is approximately 50% of that of the peak wavelength. In addition, when manufacturing LEDs, it is difficult to tightly control the mean wavelength. Thus, a purchaser specifying a particular wavelength, such as a 735 nm wavelength in an embodiment of the present invention, will expect to receive LEDs whose actual mean wavelength can vary by 10, 20 or more nanometers from the specified value. A narrow range is typically achieved by testing and sorting.

FIG. **27** is a block diagram of one embodiment of a pulse oximeter implementing the present invention. Light from light source **210** passes into patient tissue **212**, and is scattered and detected by photodetector **214**. A sensor **200** containing the light source and photodetector may also contain an encoder **216** which provides signals indicative of the wavelength of light source **210** to allow the oximeter to select appropriate calibration coefficients for calculating oxygen saturation. Encoder **216** may, for instance, be a resistor.

Sensor **200** is connected to a pulse oximeter **220**. The oximeter includes a microprocessor **222** connected to an internal bus **224**. Also connected to the bus is a RAM memory **226** and a display **228**. A time processing unit (TPU) **230** provides timing control signals to light drive circuitry **232** which controls when light source **210** is illuminated, and if multiple light sources are used, the multiplexed timing for the different light sources. TPU **230** also controls the gating-in of signals from photodetector **214** through an amplifier **233** and a switching circuit **234**. These signals are sampled at the proper time, depending upon which of multiple light sources is illuminated, if multiple light sources are used. The received signal is passed through an amplifier **236**, a low pass filter **238**, and an analog-to-digital converter **240**. The digital data is then stored in a queued serial module (QSM) **242**, for later downloading to RAM **26** as QSM **242** fills up. In one-embodiment, there may be multiple parallel paths of separate amplifier filter and A/D converters for multiple light wavelengths or spectrums received.

A detector and decoder module **242** determines the wavelength of the light source from encoder **216**. One embodiment of circuitry for accomplishing this is shown in commonly assigned U.S. Pat. No. 4,770,179, the disclosure of which is hereby incorporated by reference.

Based on the value of the received signals corresponding to the light received by photodetector **214**, microprocessor **222** will calculate the oxygen saturation using well-known algorithms. These algorithms require coefficients, which may be empirically determined, corresponding to, for example, the wavelengths of light used. These are stored in a ROM **246**. The particular set of coefficients chosen for any pair of wavelength spectrums is determined by the value indicated by encoder **216** corresponding to a particular light source in a particular sensor **200**. In one embodiment, multiple resistor values may be assigned to select different sets of coefficients. In another embodiment, the same resistors are used to select from among the coefficients appropriate for an infrared source paired with either a near red source or far red source. The selection between whether the near red or far red set will be chosen can be selected with a control input from control inputs **254**. Control inputs **254** may be, for instance, a switch on the pulse oximeter, a keyboard, or a port providing instructions from a remote host computer.

The inventors of the present invention use both modeling and prototypes to achieve the optimized sensor set forth herein. Several theoretical models exist for describing the scattering of light within tissue. The models used by the inventors assume isotropic scattering within a homogeneous tissue bed. Even though this is a simplification of the true nature of light scattering in tissue (tissue is inhomogeneous and light is scattered primarily in the forward direction), these models are useful for predicting behaviors of pulse oximetry, and the sensitivity to many design parameters.

Utilizing such a model, different choices of LED wavelengths were explored. Tissue characteristics were numerically defined and the basis (calibration) correlation between SaO_2 and modulation ratio was calculated for each wavelength pair considered. Change in physiological condition was simulated by revising one or more of the numerically defined physical parameters. SpO_2 was recalculated from the resulting modulation ratio, and the saturation region where errors were minimized was noted. For arterial saturations above 80% the conventional wavelength choice of 660 nm paired with 890 nm results in optimum performance, while for arterial saturations below 70%, 735 nm band emitters paired with 890 nm gives improved stability.

FIGS. **7** through **18** show the predicted errors due to changing the tissue blood volume to one fourth the basis value for a variety of red and IR LED wavelength pairs. The A figures (such as **7**A) show the modulation ratio vs. SaO_2. The B figures (**7**B) show the saturation error vs. SaO_2. This perturbation simulates the effects of blood volume variations within the patient population, anemia, ischemia, or localized exsanguination of blood in the tissue.

Sensitivity of the calibration to a change in tissue blood concentration is shown for several pairings of red and IR wavelengths. In each case, the LED has no secondary emission, and the perturbation is in going from a nominal 2% blood concentration in the tissue to 0.5%.

Figure Table

	IR LED		
red LED	805 nm	890 nm	940 nm
660 nm	7	8	9
700 nm		10	
730 nm	11	12	13
760 nm	14	15	16
790 nm		17	18

FIGS. **7–9** show the type of performance found in conventional pulse oximeters. FIGS. **10–18** show shifting of the optimum performance region from saturations above 80% to lower saturations when the red LED wavelength is chosen in the 700 nm–790 nm region of the spectrum. Light scattering is minimally affected by changes in oxygenation, but light

absorption is significantly affected as reduced hemoglobin in the tissue changes to oxyhemoglobin or vice-versa. Pulse oximetry's optimum performance region occurs when there is a balance of the two channels' scattering and absorption properties within blood perfused tissue. Balance occurs when there is a good overlap of the volumes of tissue probed by the two channels, requiring that the penetration depth of light at the two wavelengths be matched. At the higher saturations, this optimum balance occurs with the pairing of wavelengths with a red emitter in the 660 nm band, while at the lower saturations the balance improves with the use of a red emitter in the 730 nm band. The variation of the IR LED from 805 to 940 nm does not produce a significant difference in performance.

When using an LED pair near 730 nm and 890 nm for pulse oximetry, the sensitivity of modulation ratio to changes in oxygen saturation (i.e., the slope of the curve in, for example, FIG. **1**) is reduced relative to the use of 660 nm and 890 nm, but the measurement becomes more robust to changes in the tissue characteristics other than oxygen saturation. Noise in the measurement of modulation ratio due to factors such as instrument electronics noise, digitization, or ambient light interference, become more important but can generally be accounted for with good instrument design and appropriate signal processing. The bias and deviations due to tissue optical properties, however, become less significant with the proper choice of emitter wavelengths when they are chosen based on the saturation region of primary interest.

The inventors conducted empirical tests on sheep using prototype sensors. The empirical observations support the use of 735 nm band red LEDs in the design of a pulse oximeter that is more robust to perturbation induced artifacts at the lower saturation region. Reflectance pulse oximetry sensors were fabricated using conventional 660 nm–890 nm LED pairs, and with 735 nm–890 nm pairs.

FIGS. **19–23** show that measurements were taken at a range of oxygen saturation values indicated along the X axis from approximately 100% oxygen saturation to less than 10%. The plots show the calculated saturation (SpO_2) for each actual saturation (SaO_2) value. The actual saturation value is determined by simultaneously drawing blood samples from an arterial catheter placed in the left femoral artery. SaO_2 is measured on a laboratory co-oximeter (Instrument Labs IL 282 or Radiometer OSM-3). This is the value used on the X axis in these figures.

As can be seen, the diagonal line in FIGS. **19**, **20**, and **22** indicates the desired result where the calculated value is equal to the actual value as measured with the catheter. The tests illustrated in FIGS. **19**, **20**, and **22** were done with a nominal force of approximately 50 grams applied to the sensor holding it against the skin.

Using the 660 nm sensor with center-to-center emitter/detector spacing of 14 mm at the tissue, FIG. **19** shows that sensor calibration is very sensitive to the type of tissue probed. The calibration on the head and neck are very different.

Using the 735 nm sensor with a 5.8 mm center-to-center emitter/detector spacing at the tissue, the bias between the head and neck is greatly reduced as illustrated by FIG. **20**. There is, however, still substantial sensitivity to surface exsanguination. This is apparent in FIG. **21** which illustrates the effect of a perturbation induced artifact (sensor applied force).

FIG. **22** shows the location insensitivity of a 735 nm sensor with a 14 mm center-to-center emitter/detector spacing. FIG. **23** shows that this sensor is also insensitive to force applied to the sensor (perturbation induced artifact).

It was experimentally confirmed that increasing the emitter/detector center-to-center spacing from 5.8 mm for 735 nm/890 nm LED wavelengths decreased the sensitivity to perturbation induced artifacts, with good performance being achieved by an emitter/detector separation equal to or greater than 10 mm.

Both the modeling and the actual experiments illustrate an improvement in reliability of a saturation measurement achieved by optimizing the red wavelength to be within 700–790 nm range. In addition, reduction of the saturation error reading in the presence of force artifact is achieved by increasing the spacing of the emitters from the detector.

The force applied to the sensor causes exsanguination of the surface tissue, further magnifying the remaining disparities due to the inhomogeneity of the tissue, or causing shunting of light between the emitter and detector, thus causing errors in the saturation calculation. These are compensated for by wider emitter/detector spacing, which results in the light from the red and infrared LEDs penetrating deeper into the tissue, thus increasing the likelihood of their going through, on the average, the same combination of tissue structures, as illustrated in FIG. **3**.

FIG. **24** is a top view of a sensor according to one embodiment of the present invention. The sensor face **110** supports a far red LED **112** and an infrared LED **114**. These are spaced by a distance of 14 mm center-to-center from a detector **116**. Preferably, the centers of the far red and infrared LEDs are no more than 0.5 mm apart. The sensor face is connected by a cable **118** to a connector **120** for connection to the pulse oximeter monitor. FIG. **25** shows a side view of the sensor of FIG. **24**, illustrating the fulcrum portion **122** of the sensor and sensor back **132**. When placed in utero, the uterus will apply a force to the sensor back **132** and deform the fulcrum **122**. As can be seen, this technique results in a force being applied to the sensor resulting in good sensor-fetus contact but possibly resulting in local exsanguination of the tissue. It should be noted that any sensor embodiment will have possible local exsanguination.

The modeling and empirical tests show that the nature of the correlation between modulation ratio and saturation in pulse oximetry is related to tissue optical properties, and that the sensitivity to varying perturbation induced artifacts can be affected by choice of emitter wavelengths. For high oxygen saturations, the choice of 660 nm and 890 nm band emitters is well suited for stable pulse oximetry calculations, while 700–790 nm and 890 nm band emitters perform better at low saturations. Other wavelength combinations may be chosen from elsewhere in the visible and near infrared portion of the spectrum by following an analysis similar to the one described here. Currently, however, overall instrument design considerations (e.g., electronic signal-to-noise and potential shunting of light with narrowly spaced components in a reflectance probe) favor the use of the wavelengths discussed. By using the analysis described, other improvements to pulse oximetry are possible. FIGS. **19–23** illustrate the results of these tests for several prototype sensors.

FIGS. **26**A and **26**B are front and side views of a single package containing emitters **112** and **114** of FIGS. **24** and **25**. Both emitters are encapsulated in a single semiconductor package, to make the package more compact to provide the miniaturization which is advantageous for a fetal sensor application. In the embodiment of FIG. **26**A, emitter die **112** is mounted via a conductive epoxy **130** to a substrate **132**.

Substrate **132** takes the form of a metal plating, an exterior portion **134** of which forms the outside lead to the package. Emitter **114** is mounted on top of metal substrate **136**, an exterior **138** of which forms the second lead.

The electrical connection to emitter **114** is provided through lead **138** on one side up through the conductive epoxy, and through the other side via a wire bond **140**, which connects to the other lead **134**. Similarly, lead **134** connects through conductive epoxy **130** to the second emitter **112**, with the other side of emitter **112** connected via a wire bond **142** to lead **138**. Accordingly, as can be seen, applying a voltage with a first polarity to the two leads **134** and **138** will turn on one of the emitters, and turn off the other, while reversing the polarity will reverse which emitter is turned on and which emitter is turned off. Both of the emitters and their corresponding substrates are encapsulated in a package **144** which may, for instance, be plastic.

FIG. **26**B is a side view showing the encapsulated package **144** from the side, and illustrating the emitting light **146** from emitters **112**, **114**. The structure of FIGS. **26**A–**26**B is compact and usable for a fetal application. Preferably, the distance between the centers of the two emitter dies **112** and **114** is less than 2 mm. This way the package's wiring allows the package to have two leads, as opposed to four leads which would be required by using two separate emitter packages.

As an alternative to using a far red and an infrared LED, other methods for producing selected light spectrums of two different wavelengths can be used. For example, lasers could be used rather than LEDs. Alternately, a white light or other light source could be used, with the wavelength being optimized at the detector. This could be done by using appropriate filters in front of either the light source or the detector, or by using a wavelength sensitive detector. If filters are used, they could be placed in front of alternate detectors or emitters, or filters could be alternately activated in front of a single emitter or detector.

A pulse oximeter for use over a broad saturation range can utilize multiple wavelength pairs (e.g., both 660 nm and 730 nm band emitters coupled with a 900 nm-emitter), with the appropriate emitter pair chosen for use in the calculation of SpO_2 based on the estimated value of the oxygen saturation.

Such a pulse oximeter could be implemented with two or more red LEDs, or alternately could be implemented with a single light source and multiple filters, or multiple wavelength sensitive detectors. Different red wavelength spectrums could be utilized, based on the saturation of the patient.

As will be understood by those with skill in the art, the present invention can be embodied in other specific forms without departing from the essential characteristics thereof. The wavelength could be varied while still optimizing in accordance with the present invention. Also, light pipes, light fibers, multiple filters, or multiple detectors could be used in accordance with the concepts of the present invention. Different sensors than the fulcrum structure as set forth in FIG. **25** could be used, such as a bladder structure for inflating and holding the sensor against the fetus. Accordingly, reference should be made to the appended claims for defining the scope of the invention.

What is claimed is:

1. A method for measuring blood oxygen saturation in a fetus, comprising the steps of:

providing a sensor and a pulse oximeter;

selecting a far red and infrared light source and a light detector;

detecting light at said detector including an infrared wavelength spectrum useful for measuring oxygen saturation in a patient with high saturation, the detected light including a far red wavelength spectrum which has a mean wavelength between 700 and 790 nanometers;

placing said light sources in a single encapsulated package and mounting said package on said sensor;

placing said sensor on said fetus;

measuring an intensity of light from said light source at said light detector after scattering through a portion of said fetus; and

determining said blood oxygen saturation using said intensity and said pulse oximeter.

2. The method of claim **1** further comprising the steps of:

selecting a second red light source;

selecting a wavelength spectrum of said second red light source to have a mean wavelength less than 700 nanometers; and

selectively activating either or both said first mentioned or second red light source.

3. A fetal pulse oximeter sensor comprising:

a housing;

at least one light source mounted in said housing;

at least one detector mounted in said housing;

means for detecting light subsequent to being scattered by fetal tissue, the light including an infrared light spectrum, said infrared spectrum having a range useful for measuring oxygen saturation in a patient with high saturation, the detected light also including a red light spectrum, said red light spectrum having a mean wavelength between 700 and 790 nanometers;

said detector being mounted in said housing spaced from said light sources and positioned to detect light from said light sources; and

in which the combination of the light source and detector limit light signals received at the detector from the light source to no more than three spectra.

4. The sensor of claim **3** wherein said light source comprises at least one LED.

5. The sensor of claim **3** wherein said light source comprises red and infrared light sources spaced from said detector by at least 10 mm.

6. The sensor of claim **3** wherein said light source comprises red and infrared light sources spaced from said detector by at least 14 mm.

7. The sensor of claim **3** wherein said means for providing comprises a light source which emits a limited spectrum.

8. The sensor of claim **3** wherein said means for providing comprises a filter between said light source and said detector for passing a limited spectrum of light.

9. The sensor of claim **3** wherein said means for providing comprises a wavelength sensitive detector which detects a limited spectrum of light.

10. The sensor of claim **3** further comprising:

means for providing a red light spectrum having a mean wavelength less than 700 nanometers.

11. The sensor of claim **10** wherein

said means for providing a red light spectrum having a mean wavelength between 700 and 790 nanometers is a first light emitting diode; and

said means for providing a red light spectrum having a mean wavelength less than 700 nanometers is a second light emitting diode.

12. A fetal pulse oximeter comprising:

an input connector for receiving at least first and second signals from a sensor obtained by scattering light through tissue of a fetus, the light having at least red and infrared spectrums and being limited to more than three spectra;

a memory storing coefficients suitable for said infrared spectrum having a range useful for measuring oxygen saturation in a patient with high saturation and said red light spectrum having a mean wavelength between 700 and 790 nanometers; and

a processor, coupled to said memory and said input connector, for calculating the oxygen saturation of said fetus using said coefficients.

13. The pulse oximeter of claim 12 wherein said memory further comprises:

coefficients for a red light spectrum having a mean wavelength less than 700 nanometers.

14. A fetal pulse oximeter sensor which comprises a housing with at least one light source and at least one light detector mounted in the housing in such a way that the detector is spaced from the light source and can detect light from the light source after scattering by fetal tissue, in which the combination of the light source and the light detector limit light signals received at the detector from the light source to no more than three spectra, a first spectrum including 735 nanometers at an intensity of at least 50% of the intensity of any other wavelengths in said first spectrum.

15. The sensor of claim 14, wherein a second spectrum has a mean wavelength of from 805 to 940 nm used, in conjunction with said first spectrum, for measuring oxygen saturation in a patient, said sensor being connectable to a pulse oximeter for using said first and second spectra to calculate arterial oxygen saturation.

16. A sensor as claimed in claim 14 in which a third spectrum has a mean wavelength near 660 nm.

17. The sensor of claim 14 wherein said sensor is a reflectance sensor.

18. The sensor of claim 14 wherein said sensor is a transmission sensor.

19. The sensor of claim 14 wherein said light source and said light detector are spaced apart by at least 10 cm.

20. The sensor of claim 14 wherein said light source and said light detector are spaced apart by at least 14 cm.

21. The sensor of claim 14 wherein only a single said light detector is provided in said sensor.

* * * * *